Electronic and Magnetic Properties of Doped Silicon Carbide Nanosheet Under an External Electric Field

Mohammad A. Salem[1] · Jamal A. Talla[1] · Alaa L. Al-Moumani[1]

Abstract

The electronic and magnetic properties of silicon carbide nanosheets were investigated in this study, with particular attention given to the effects of doping with transition metal atoms and applying an external electric field. Our findings point out that introducing dopants, such as Mn, Co, and Zn, can notably reduce the band gap of the pristine structure from 2.6 eV to 0.752 eV, 0.261 eV, and 0.898 eV, respectively. Moreover, the inclusion of Mn and Co dopants results in magnetization. On the other hand, applying a transverse external electric field up to 7 V/nm leads to a semiconductor-to-metal phase transition. Although the applied electric field has a minor effect on the Mn-doped structure's magnetic moment, it slightly decreases the magnetic moment of the magnetized Co-doped one.

1 Introduction

The dawn of nanotechnology has witnessed the exploration of various materials at the atomic scale, unveiling their extraordinary properties and potential applications. Among these materials, two-dimensional (2D) nanosheet structures have gained significant attention due to their remarkable electronic, optical, and mechanical properties [1–5]. In general, 2D nanosheets are ultra-thin, layered materials with a thickness of just a few nanometers. These nanosheets exhibit unique properties distinct from their bulk counterparts due to their reduced dimensionality. The relatively large surface area of 2D nanosheets provides more active sites for chemical reactions, making them attractive for catalytic applications [4–7]. Since the 2D nanosheets are extremely thin, they are flexible and lightweight. However, they also exhibit high strength and rigidity, making them ideal for various applications [4,

✉ Jamal A. Talla
    jtalla@aabu.edu.jo

1   Department of Physics, Al al-Bayt University, Al-Mafraq 130040, Jordan

8]. In addition to their large surface area, 2D nanosheets show distinctive electronic properties that make them attractive for use in electronics [9–12].

Graphene, the first 2D material found, attracted considerable attention and has become the poster child for such materials [13, 14]. Recently, various 2D structures have been discovered due to searches for different materials with unique properties and improved performance. Among them is silicon carbide, the focus of this research, which has excellent potential for several applications, especially in nanoelectronics, optoelectronics, and sensors [15, 16]. The 2D silicon carbide nanosheet, also known as 2D-SiCNS, is a novel nanomaterial class recently attracting significant attention [17–20]. It is a single layer of silicon (Si) and carbon (C) atoms in a 1:1 ratio arranged in a hexagonal lattice structure. Unlike graphene, the zero-band gap semiconductor, the 2D-SiCNS exhibits a finite band gap that can be tuned by varying the thickness, strain, chemical doping, or even creating vacancies [21–23]. Theoretical and experimental studies have shown that the band gap of SiCNS ranges from 2.0 eV to 3.0 eV, making them fit for optoelectronic and electronic devices operating at high temperatures, voltages, and frequencies [21, 24].

The 2D-SiCNS can be synthesized using different techniques such as chemical vapor deposition (CVD), mechanical exfoliation, and sonication-assisted liquid-phase exfoliation [7, 25, 26]. The desired properties of the resulting SiCNS, such as their thickness, size, and quality, are considered when selecting a synthesis method. In recent years, a new approach has been developed to synthesize highly efficient and scalable precursors of SiCNS from heat decomposition at high temperatures [6].

The unique characteristics of 2D-SiCNSs make them attractive for several applications, such as hydrogen storage, catalytic converters, and optoelectronics [27]. Also, they are chemically inert, thermally stable, and resistant to oxidation, making them ideal for high-temperature applications [23]. In addition, SiCNSs have excellent mechanical properties, such as their high stiffness, strength, and fracture toughness, making them fit for structural applications [28, 29].

Moreover, SiCNSs have a wide band gap in which their electricity can only be generated if exposed to high-energy photons or electrons [30]. This property makes them appropriate for electronic devices requiring high power and temperature stability. Also, the wide band gap lets them emit and absorb light in the ultraviolet (UV) range, making SiCNSs an ideal candidate for UV detectors, light-emitting diodes, and other optoelectronic devices [11, 26]. In addition, excellent electrochemical performance and the wide surface area of the 2D-SiCNSs provides more effective energy storage [31], making them attractive for battery applications and other energy storage devices. Also, the high surface area enables efficient charge transfer and facilitates chemical reactions, making the SiCNSs attractive for use in heterogeneous catalysis [32].

Overall, the 2D-SiCNSs are an attractive material for various applications. However, fully understanding and optimizing their potential application in different fields require further research and investigation. In this study, the properties of 2D-SiCNSs have been explored, with a particular focus on the effects of doping with transition metal (TM) atoms and applying an external electric field.

2 Methodology and Structural Properties

The scope of this study is limited to investigating the changes in the electronic and magnetic properties of 2D-SiCNS resulting from the introduction of TM atoms under the influence of an external electric field. The investigation is commenced by modeling a 7×7 supercell of 2D-SiCNS using the Cambridge Serial Total Energy Package (CASTEP) code [15, 33]. A schematic representation of the modeled structure, including bond lengths and angles, and a cross-sectional view of the same structure is shown in Fig. 1a. Akin to graphene, the 2D-SiCNS structure exhibits high symmetry and features a planar honeycomb lattice configuration with alternating Si and C atoms in both (x) and (y) directions, as displayed in Fig. 1a. The robust covalent bonds between Si and C atoms enhance the material's stability as a single-atom-thick sheet.

Each unit cell in the hexagonal pattern in Fig. 1a comprises Si and C atoms, with each atom being surrounded by three atoms of the opposite type. The Si-C bond lengths in the hexagonal sheet of SiC are approximately 1.77 Å, and the angles of C–Si–C and Si–C–Si are equal to 120°. Also, the hexagonal arrangement results in two lattice constants, "a" and "b," along the (x) and (y) directions, representing the distances between neighboring atoms in the lattice. In the 2D-SiCNS structure, the lattice constants "a" and "b" are set to be the same for the SiCNS [34, 35]. Along the (z) direction, the lattice constant "c" is set large enough to avoid potential interaction between the modeled SiCNS and its image formed by the periodic boundary conditions of the simulation [34, 35].

The equal lattice constants and the hexagonal arrangement of atoms create a six-fold rotational symmetry around the axis perpendicular to the monolayer plane. A key feature of the 2D-SiCNS is its full sp2 hybridization, which enables the formation of in-plane strong σ bonds and a completely conjugated π electron system [36]. This full sp^2 hybridization arises from the Si and C atoms in the lattice sharing electrons, forming covalent bonds between
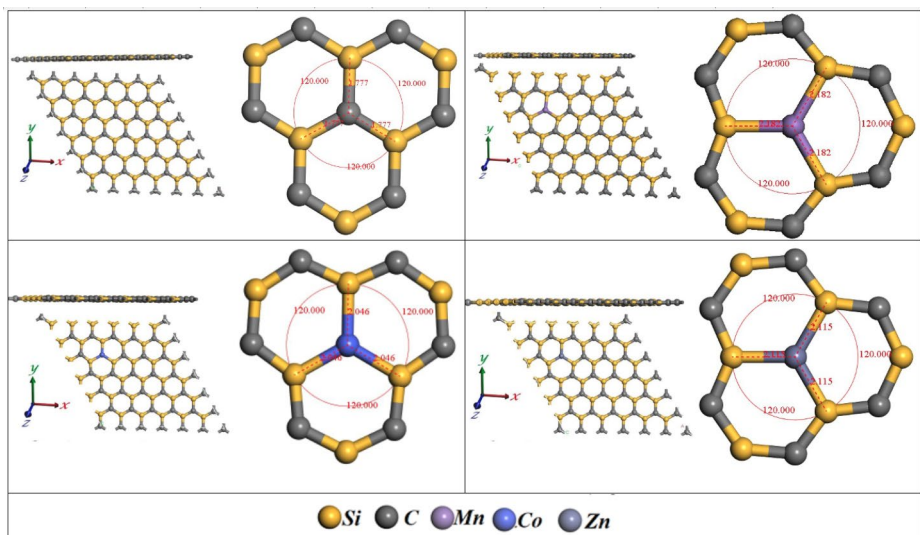

Fig. 1 Schematic diagram, bond lengths and angles, and a cross-sectional view of **a** the pristine and doped 2D-SiCNC with **b** Mn, **c** Co, and **d** Zn

each other [36]. This results in remarkable mechanical strength, thermal stability, and electrical conductivity of the 2D-SiCNS [37]. The next stage in the study involves doping the 2D-SiCNS with TM atoms. We opted to introduce atoms such as Mn, Co, and Zn into the structure, as these elements have been shown to exhibit interesting electronic and magnetic properties. The doping is done by replacing one of the C atoms with a transition metal atom in the 7×7 supercell of the 2D-SiCNS. This doping technique is commonly used in computational studies to investigate the effect of impurities on the material's properties. The newly created TM-doped 2D-SiCNS structures are depicted in Fig. 1b–d. As shown, the local environment around the doping site undergoes alterations in bond lengths since TM atoms typically possess different atomic radii and electronegativity values compared to C and Si atoms [38]. As a result, when incorporated into the SiCNS, the bond lengths between Mn, Co, and Zn atoms and the neighboring Si atoms expand to 1.82 Å, 2.046 Å, and 2.115 Å, respectively. Nevertheless, these modifications in bond lengths do not influence bond angles near the TM atom, which accounts for the absence of any protrusions in the cross-sectional view [39–41].

It is worth mentioning that all the generated structures undergo full optimization using the generalized gradient approximation (GGA) with a revised Perdew–Burke–Ernzerhof (RPBE) parameterization, with force acting on each atom limited to less than 0.1 eV/nm [13, 42, 43]. This study hopes to gain a more thorough understanding of the effects of external fields on doped nanosheets, as elaborated in the ensuing discussion.

3   Results and Discussion

In this study, both pristine and M-doped structures undergo a systematic application of an external electric field with a maximum strength of 7 V/nm. The electric field is applied perpendicular to the surface of the nanosheet structure in both positive ($+z$) and negative ($-z$) directions, which are correspondingly referred to as positive and negative fields. After that, energy calculations were conducted to monitor variations in the band structure and density of states (DOS) for all optimized geometries.

3.1   Electronic Properties

The electronic properties of 2D-SiCNS are primarily defined by the formation of energy band structure, particularly the band gap, which is a crucial feature of semiconducting materials due to its impact on their electronic performance. The energy bands and distribution of energy states (DOS) for the pristine and the TM-doped structures are depicted in Figs. 2a–c. Generally, the specific energy band structure and DOS depend on the distinctive atomic arrangement and bonding characteristics in the given structure. The energy bands represent the allowed energy levels for electrons and are constructed due to the periodic arrangement of atoms in the structure. In a simplified picture, the energy bands can be classified as valence and conduction bands. The valence band is the highest energy band loaded with electrons at absolute zero temperature, while the conduction band lies above the valence band and usually is empty or partially filled with electrons. The DOS measures the number of available energy states per unit volume at a given energy level. It provides information about the electronic structure of a material, including the distribution of energy states
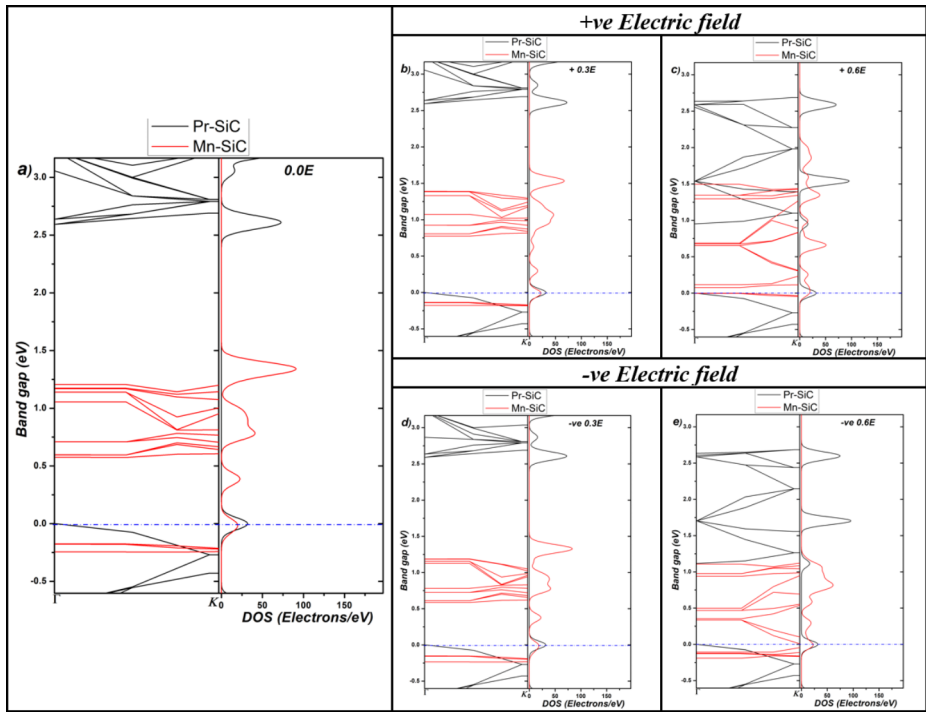
Fig. 2a Energy bands and the corresponding DOS for the Pristine (black) and Mn-doped (red) 2D-SiCNC at 0E (left pan), +3E and +6E (upper right pans), and −3E and −6E (lower right pans). The blue dotted line is the Fermi level

within the energy bands. The band gap refers to the energy separation between the valence and conduction bands that encloses the Fermi level in the energy band structure and DOS plots. As shown in left pan of Figs. 2a–c, the pristine 2D-SiCNS exhibits a relatively wide band gap of about 2.6 eV, consistent with the theoretical and experimental findings in the existing literature [29]. Nevertheless, the introduction of TM atoms significantly alters this band gap. The red curves in the left pan of Figs. 2a–c indicate that the band gap narrows to 0.752 eV, 0.261 eV, and 0.898 eV when Mn, Co, and Zn specifically replace the C atom in the 2D-SiCNS, respectively. Interestingly, our research reveals no impact on the band gap when these TM atoms are used to substitute the Si atom within the 2D-SiCNS structure.

The narrowing of the band gap is ascribed to the creation of impurity states (the new red curves) within the band gap at the top of the valence band and the bottom of the conduction band, as seen in the left pan of Figs. 2a–c. The d-orbitals of the TM atoms have the potential to hybridize with the orbitals of Si and C, creating new energy bands. The extent of this hybridization is contingent upon the specific TM atoms and their interaction with the SiCNS lattice structure. The development of hybridized orbitals can result in the redistribution of electronic states, which subsequently alters the band gap of the 2D-SiCNS. Additionally, introducing TM atoms within the 2D-SiCNS can transfer charge between the TM atoms and the SiCNS lattice. This charge transfer has the potential to induce a displacement in the Fermi level, which could cause the energy bands to shift and ultimately result in a modification of the band gap. The extent of charge transfer and its influence on the band gap depends
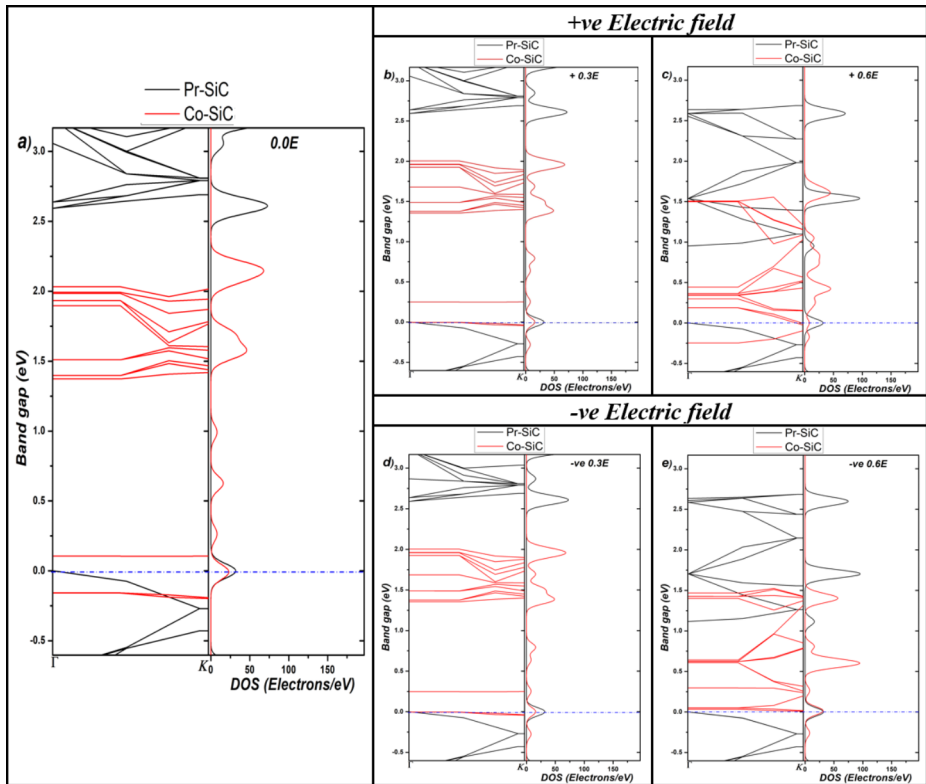
Fig. 2b Energy bands and the corresponding DOS for the Pristine (black) and Co-doped (red) 2D-SiCNC at 0E (left pan), +3E and +6E (upper right pans), and −3E and −6E (lower right pans). The blue dotted line is the Fermi level

on the difference in electronegativity between the TM atoms and SiC and the oxidation states of the TM atoms [44]. In order to gain an understanding of the interactions between atoms and the transfer of electrons, Fig. 3 displays the Hirshfeld electron density difference distribution for bonding atoms in the pristine and TM-doped SiCNS structures. The electron density is depicted using a color scheme, where the higher electron density is represented by blue, and red signifies regions with lower electron density. In the pristine SiCNS structure (Fig. 3a), the electron distribution is uniform around the C atom, consistent with its electronegativity. However, when the C atom is replaced by a transition metal (TM) atom, the electron density distribution around the replaced atom changes, as shown in Fig. 3b–d. The size of the blue regions around the TM atom decreases, indicating a reduction in electron density. Conversely, the blue regions around the neighboring Si atoms expand, indicating an increase in electron density. These changes in electron density distribution suggest that electron transfer occurs from the TM atoms to the Si atom in the TM-doped SiCNC structure, resulting in an electron transfer phenomenon.

Moreover, incorporating TM atoms into the SiCNS lattice structure can induce a tensile strain. This strain arises from the significant difference in atomic size and bond length between the TM on the one hand and Si and C atoms on the other hand. When TM atoms
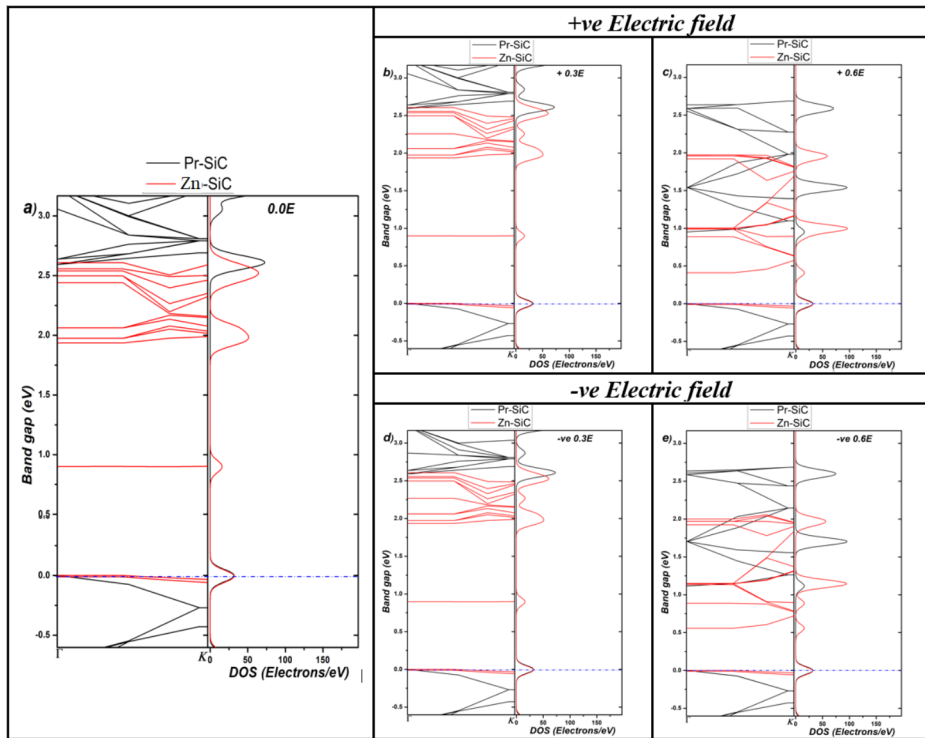
Fig. 2c Energy bands and the corresponding DOS for the Pristine (black) and Zn-doped (red) 2D-SiCNC at 0E (left pan), +3E and +6E (upper right pans), and −3E and −6E (lower right pans). The blue dotted line is the Fermi level

are introduced into the lattice, their larger size and different bonding characteristics cause the structure to stretch or experience tension. This strain can be visualized as a deformation of the SiCNC lattice structure, depicted in Fig. 1b, c. The strain-induced deformation of the lattice structure alters the electronic structure and energy bands of the 2D-SiCNS and modifies the band gap.

On the other hand, the findings of this study indicate that the band gap of the pristine and TM-doped 2D-SiCNS is further reduced upon applying a transverse external electric field of value ranges between 0 and 7 V/nm. However, our results show that an electric field of values greater than 7 V/nm results in a structural deformation. The variation in the band gap under the applied external electric field in both positive and negative directions is illustrated in Fig. 4. The dark shade of each color indicates the positive field, while the light shade represents the negative field. As shown from the dark shade, the band gap of the pristine and TM-doped 2D-SiCNS is gradually decreasing as the positive external electric field increases in the range between 1 and 5 V/nm. However, the band gap is steeply reduced, and a semiconductor-metal phase transition occurs under the influence of an electric field ranging between 5 and 7 V/nm. The band gap of the pristine and TM-doped 2D-SiCNS behaves almost the same upon applying a negative external electric field, as shown from the light shade in Fig. 4.
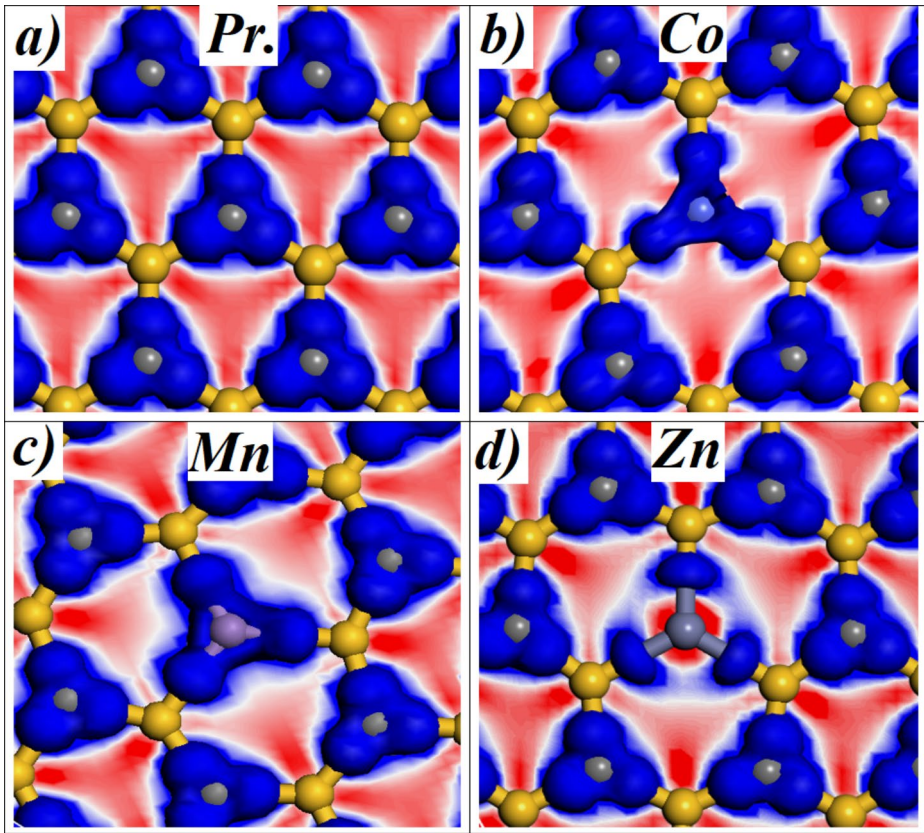
Fig. 3 Electron density distribution for **a** pristine and the doped 2D-SiCNC with **b** Mn, **c** Co, and **d** Zn. The blue represents higher electron density, and the red indicates lower density

The reduction in the band gap of the pristine 2D-SiCNS, under the influence of an external electric field, can generally be justified by the Stark effect [45]. This effect occurs when the electric field causes the energy levels of the valence and conduction bands to split and shift in opposite directions. Specifically, the electric field increases the valence band's energy while decreasing the conduction band's energy. Consequently, the band gap is reduced, allowing electrons to transition more easily from the valence band to the conduction band [11, 13, 39]. Accordingly, the material exhibits enhanced conductivity when subjected to the electric field. It is important to note that the response of the band gap to the external electric field can also be influenced by other factors, such as doping, which interact with the electric field and further modify the band gap. In the TM-doped 2D-SiCNS, the Stark effect causes the impurity states to shift the energy in response to the electric field. The impurity states are localized around the TM atoms and interact strongly with the electric field. As a result, the impurity states energy shift, reducing the band gap (refer to Figs. 2a and c are examples of the created impurity states at $\pm$ 3E and $\pm$ 6E). The extent of the reduction depends on the strength, direction of the applied external electric field, and the type of the TM atom, as predicted in Fig. 4. Also, the interaction between the external electric field and the dopant atom can lead to a change in its oxidation state. For example, a TM atom with a positive
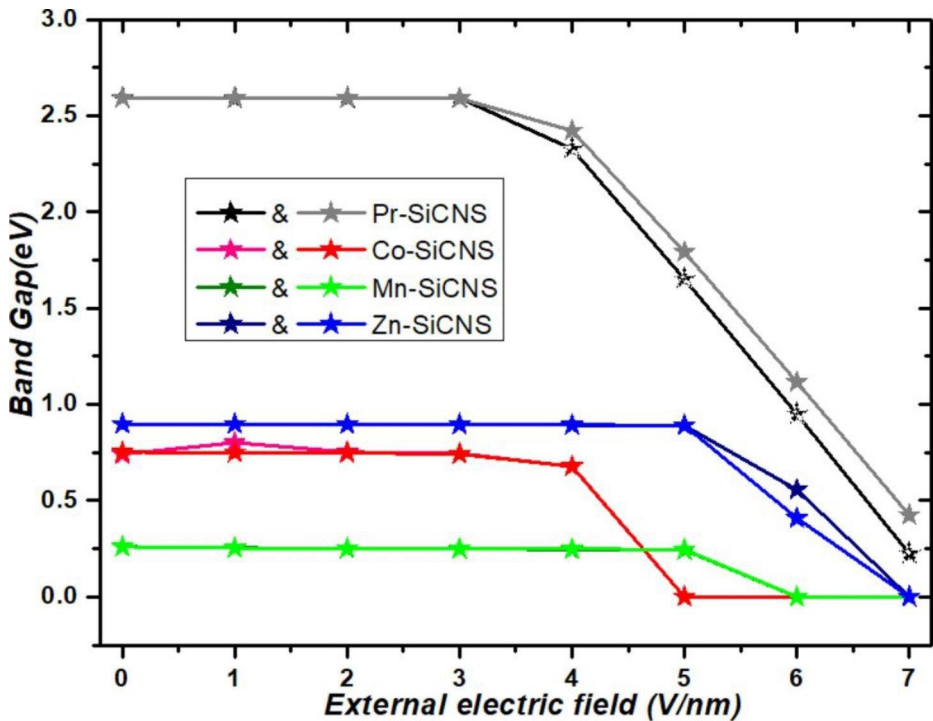
Fig. 4 The variation in the bandgap with positive (the dark shade of each color) and negative (the light shade of each color) applied external electric field on the pristine and Co, Mn, and Zn-doped 2D-SiCNC

oxidation state can be reduced to a lower oxidation state under the influence of the electric field. This change in oxidation state can affect the electronic configuration of the dopant atom, leading to a change in its bonding with the surrounding atoms and hence the band gap of the 2D-SiCNS structure. In addition to the change in oxidation state, the interaction between the external electric field and the dopant atom can also affect the position of the localized states within the band gap [46–49]. For example, a positively charged TM atom may be attracted to the negatively charged side of the electric field, causing the localized states to move toward the conduction band. This movement of the states can reduce the effective band gap of the 2D-SiCNS structure, making it easier for electrons to be excited to the conduction band.

3.2 Magnetic Properties

Generally, the number of spin-up and spin-down electrons in any material with magnetic properties is imbalanced. This imbalance results from a net magnetic effect directly showing the material's magnetic properties. Usually, the DOS is a crucial concept in understanding the magnetic properties, as it provides information about the distribution of electron states in a material at various energy levels, thus allowing for the examination of spin-polarized electron states. Before applying an external electric field, Fig. 5a shows that the DOS of the pristine SiCNS structure is characterized by symmetric spin-up and spin-down curves, indi-
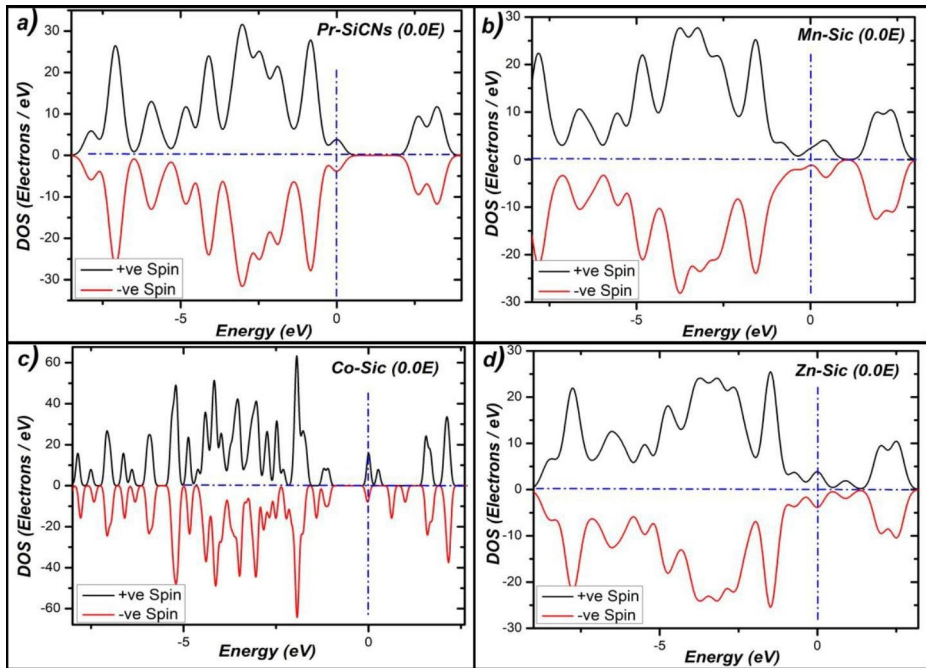
Fig. 5 DOS at zero electric fields for **a** the pristine and doped 2D-SiCNC with **b** Mn, **c** Co, and **d** Zn. The black line represents the spin-up DOS, and the red line represents the spin-down DOS

cating the absence of intrinsic magnetic properties. The symmetry in the DOS curves is due to the absence of unpaired electron spins in the pristine SiCNS structure, in which C and Si atoms have filled outer electron shells, leading to a stable and non-magnetic configuration. Despite being considered non-magnetic materials, it has been found that introducing TM dopants could induce magnetic properties in SiCNS. Figure 5b, c reveal that the spin-up and spin-down DOS curves of Zn-doped structures are symmetric, while those of Mn and Co-doped structures are imbalanced. The asymmetry in DOS curves suggests that incorporating such TM atoms could introduce unpaired electrons, which can interact with the electrons in the SiCNS lattice structure. This interaction can lead to the formation of magnetic moments and, consequently, magnetism. Nevertheless, the strength of the magnetism depends on the nature of the dopant and the interaction between dopant atoms and the SiCNS lattice structure. For instance, Mn and Co-doped SiCNS exhibit ferromagnetic behavior due to the strong exchange interaction between the Mn and Co atoms and the SiCNS lattice structure due to the alignment of its magnetic moments in a parallel configuration. This interaction leads to the alignment of unpaired electron spins, resulting in a net magnetic moment of 4.499 and 1.517, respectively. However, Zn-doped SiCNS exhibit antiferromagnetic behavior, where the Zn atoms' magnetic moments are aligned in opposite directions, leading to a zero net magnetic moment [8, 50]. On the other hand, the variation of the magnetic moment for Mn and Co-doped SiCNS with the applied external electric field ranges from 1 to 7 V/ nm and in both positive and negative directions are described in Table 1. According to the table, when subjected to a positive external electric field, the magnetic moment values for Mn-doped SiCNS vary around 4.522, whereas when exposed to a negative electric field,

Table 1 The magnetic moment values for both Mn and Co-doped 2D-SiCNS under external electric field strengths range from 0 to 6 V/nm

E (V/nm)	Mn		Co	
	Positive E	Negative E	Positive E	Negative E
0	4.499	4.499	1.517	1.517
1	4.466	4.377	1.189	1.189
2	4.499	4.507	1.188	1.189
3	4.395	4.510	1.187	1.188
4	4.434	4.426	1.139	1.149
5	4.927	4.597	1.197	1.197
6	4.436	4.531	1.147	1.147

the values fluctuate around 4.492. These results suggest that the magnetic moment of Mn-doped SiCNS remains unaffected by applying an external magnetic field. This behavior can be attributed to the fact that the magnetic moment of Mn is primarily determined by the spin of the 3d electrons in the Mn atom, which is not significantly affected by external electric fields. Table 1 also shows that, when applying an external electric field, whether positive or negative, there is a slight decrease in the magnetic moment of the Co-doped SiCNS. This observation suggests that the magnetic features of the Co-doped 2D-SiCNS are tunable through the external electric field modulation of magnetism. This phenomenon is due to interactions of the magnetic moment of the Co-doped 2D-SiCNS with the external electric field, causing changes in electrons' spin orientations and, thus, a change in the magnetic moment of the structure. It is worth noting that electric field modulation of magnetism has potential applications in developing new types of electronic devices, such as spintronics, which aim to use the spin of electrons to store and process information. By controlling the magnetic properties of a material with an electric field, it is possible to create devices that can be programmed and operated electrically without the need for magnetic fields or currents.

4 Conclusion

The 2D-SiCNS is a new nanomaterial with tunable electronic and magnetic properties by doping and applying an external electric field. Substituting the C atom in the 2D-SiCNS with a TM atom like Co, Mn, and Zn can effectively modify the electronic and magnetic properties of the nanosheet. Introducing each TM atom can narrow the finite band gap of a pristine 2D-SiCNS, while only Mn and Co can magnetize the structure. However, no such effect is observed when the above-mentioned TM atoms replace the Si atom within the 2D-SiCNS structure. The impact of an external field range from 0 to 7 V/nm on the electronic and magnetic properties of the pristine and TM-doped 2D-SiCNS is also examined. The findings show that the band gap is further decreased, and a transition from semiconductor to metal occurs within an electric field range of 5 to 7 V/nm. While the magnetic moment of the Mn-doped structure is not significantly affected, the magnetized Co-doped structure experiences a slight reduction in its magnetic moment due to the applied electric field. Overall, the findings of this study demonstrate the potential of silicon carbide nanosheets as a promising platform for developing advanced electronic and magnetic materials with tailored properties for various technological applications.

Author Contributions The study conception and design was contributed by all authors. Material preparation, data collection, and analysis were carried out by MS, JT and AA. The first draft of the manuscript was written by JT and MS, and all authors provided comments on previous versions of the manuscript. The final manuscript was reviewed and approved by all authors.

Declarations

Competing Interests The authors declare no competing interests.

References

1. Talla, J.A., Msallam, Z.M.: Influence of induced ripples on optical properties of graphene: density functional theory. Russ. J. Inorg. Chem. **67**(S1), S52–S62 (2023)
2. Talla, J.A., Ahmad, M.S.: Structural and electronic Properties of Rippled Graphene monolayer: Density Functional Theory. J. Electron. Mater. **51**(5), 2464–2474 (2022)
3. Talla, J.A., Almahmoud, E.A., Al-Khaza'leh, K., Abu-Farsakh, H.: Structural and electronic properties of rippled graphene with different orientations of Stone Wales defects: first-principles study. Semiconductor **55**, 796–806 (2021)
4. Chauhan, D., Ashfaq, M., Talreja, N., Managalraja, R.V.: 2D materials for environment, energy, and biomedical applications. J. Biomed. Res. Environ. Sci. **2**(10), 977–984 (2021)
5. Thulasiraman, A.V., Ganesapillai, M.: A systematic review on the synthesis of silicon carbide: an alternative approach to valorisation of residual municipal solid waste. Processes **11**(1) (2023)
6. Kajale, S.N., Yadav, S., Cai, Y., Joy, B., Sarkar, D.: 2D material based field effect transistors and nano-electromechanical systems for sensing applications. iScience **24**(12), 103513 (2021)
7. Sulleiro, M.V., Dominguez-Alfaro, A., Alegret, N., Silvestri, A., Gómez, I.J.: 2D materials towards sensing technology: From fundamentals to applications. Sens. Bio-Sensing Res. **38** (2022)
8. Pashanova, K.I., Ershova, I.V., Trofimova, O.Y., Rumyantsev, R.V., Fukin, G.K., Bogomyakov, A.S., Arsenyev, M.V., Piskunov, A.V.: Charge transfer chromophores derived from 3d-row transition metal complexes. Molecules 27, no. 23, Nov 24 (2022)
9. Torrisi, F., Hasan, T., Wu, W., Sun, Z., Lombardo, A., Kulmala, T.S., Hsieh, G.W., Jung, S., Bonaccorso, F., Paul, P.J., Chu, D., Ferrari, A.C.: Inkjet-printed graphene electronics. ACS Nano **6**(4), 2992–3006 (2012)
10. Majid, A., Rani, N., Malik, M.F., Ahmad, N., Najam al, H., Hussain, F., Shakoor, A.: A review on transition metal doped silicon carbide. Ceram. Int. **45**(7), 8069–8080 (2019)
11. Chaves, A., Azadani, J.G., Alsalman, H., da Costa, D.R., Frisenda, R., Chaves, A.J., Song, S.H., Kim, Y.D., He, D., Zhou, J., Castellanos-Gomez, A., Peeters, F.M., Liu, Z., Hinkle, C.L., Oh, S.-H., Ye, P.D., Koester, S.J., Lee, Y.H., Avouris, P., Wang, X., Low, T.: Bandgap engineering of two-dimensional semiconductor materials. npj 2D Mater. Appl. **4**(1) (2020)
12. Talla, J.A., Salem, M.A.: Combined effect of Stone–Wales defects and titanium doping on electronic properties of a silicon carbide monolayer: DFT. J. Comput. Electron. (2022)
13. Talla, J.A.: Band gap opening of doped graphene stone wales defects: simulation study. Semiconductors **54**(1), 40–45 (2020)
14. Talla, J.A.: Pressure induced phase transition and band gap controlling in defective graphene monosheet: Density functional theory. Mater. Res. Express. **6**(11), 115012 (2019)
15. Talla, J.A.: Electronic properties of silicon carbide nanotube with Stone Wales defects under uniaxial pressure: A computational study. Comput. Condens. Matter. **19**, e00378 (2019)
16. Ghozlan, A.A., Talla, J.A.: Optical properties of defective silicon carbide nanotubes: Theoretical study. Rev. Cubana Fis. **36**, 27–36 (2019)
17. Chabi, S., Guler, Z., Brearley, A.J., Benavidez, A.D., Luk, T.S.: The creation of true two-dimensional silicon carbide. Nanomaterials (Basel) **11**(7) (2021)
18. Zhang, L., Cui, Z.: First-principles study of metal impurities in Silicon Carbide: structural, magnetic, and electronic properties. Front. Mater. **9** (2022)
19. Khan, A.A., Ahmad, R., Ahmad, I.: Silicon carbide and III-nitrides nanosheets: promising anodes for Mg-ion batteries. Mater. Chem. Phys. **257** (2021)
20. Chabi, S., Kadel, K.: Two-dimensional silicon carbide: emerging direct band gap semiconductor. Nanomaterials (Basel) **10**(11) (2020)

21. Nguyen, D.-T., Le, M.-Q.: Mechanical properties of various two-dimensional silicon carbide sheets: An atomistic study. Superlattices Microstruct. **98**, 102–115 (2016)
22. Sun, L., Wang, B., Wang, Y.: A novel silicon carbide nanosheet for high-performance humidity sensor. Adv. Mater. Interfaces **5**(6) (2018)
23. Jahanshahi, D., Ostadhassan, M., Vessally, E., Azamat, J.: Performance of silicon carbide nanomaterials in separation process. Sep. Purif. Rev. 1–16 (2022)
24. Lin, X., Lin, S., Xu, Y., Hakro, A.A., Hasan, T., Zhang, B., Yu, B., Luo, J., Li, E., Chen, H.: Ab initio study of electronic and optical behavior of two-dimensional silicon carbide. J. Mater. Chem. C **1**(11) (2013)
25. Wang, C., Song, Y., Huang, H.: Evolution application of two-dimensional MoS(2)-based field-effect transistors. Nanomaterials (Basel) **12**(18) (2022)
26. Novoselov, K.S., Mishchenko, A., Carvalho, A., Castro Neto, A.H.: 2D materials and van der Waals heterostructures. Science **353**(6298), aac9439 (2016)
27. Khan, A.A., Ahmad, A., Al-Swaidan, H.M., Haider, S., Akhtar, M.S., Khan, S.U.: Density functional theory study of P-embedded SiC monolayer as a robust metal free catalyst for N2O reduction and CO oxidation. Mol. Catal. **527** (2022)
28. Huang, L., Liu, H., Deng, X., Cui, W.: The structural, mechanical and electrical properties of 2D SiC with C-related point defects and substitution of C by foreign atoms. Vacuum **208** (2023)
29. Talla, J.A., Salem, M.A.: Combined effect of Stone–Wales defects and titanium doping on electronic properties of a silicon carbide monolayer: DFT. J. Comput. Electron. **22**, 68–79 (2023)
30. Dyck, O., Zhang, L., Yoon, M., Swett, J.L., Hensley, D., Zhang, C., Rack, P.D., Fowlkes, J.D., Lupini, A.R., Jesse, S.: Doping transition-metal atoms in graphene for atomic-scale tailoring of electronic, magnetic, and quantum topological properties. Carbon. **173**, 205–214 (2021)
31. Chen, S., Chen, Z., Xu, X., Cao, C., Xia, M., Luo, Y.: Scalable 2D mesoporous silicon nanosheets for high-performance lithium-ion battery anode. Small **14**(12), e1703361 (2018)
32. Hu, M.-S., Kuo, C.-C., Wu, C.-T., Chen, C.-W., Ang, P.K., Loh, K.P., Chen, K.-H., Chen, L.-C.: The production of SiC nanowalls sheathed with a few layers of strained graphene and their use in heterogeneous catalysis and sensing applications. Carbon **49**(14), 4911–4919 (2011)
33. Al-Khaza'leh, K., Talla, J.A., Salem, M.A.: Effect of external electric field on the electronic and magnetic properties of doped silicon carbide nanotubes: DFT. Appl. Phys. A **129**(4) (2023)
34. Nairata, M., Talla, J.: Electronic Properties of aluminum doped carbon nanotubes with Stone Wales defects: density functional theory. Phys. Solid State **61**(10), 1896–1903 (2019)
35. Almahmoud, E., Talla, J.A.: Band gap tuning in carbon doped boron nitride mono sheet with Stone-Wales defect: A simulation study. Mater. Res. Express. **6**(10), 105038 (2019)
36. Zhao, Z., Yong, Y., Zhou, Q., Kuang, Y., Li, X.: Gas-sensing properties of the SiC monolayer and bilayer: a density functional theory study. ACS Omega **5**(21), 12644–12373 (2020)
37. Sun, K., Wang, T., Gong, W., Lu, W., He, X., Eddings, E.G., Fan, M.: Synthesis and potential applications of silicon carbide nanomaterials/nanocomposites. Ceram. Int. **48**(22), 32571–32587 (2022)
38. Nejadsattari, F., Stadnik, Z.M.: Spin polarized density functional theory calculations of the electronic structure and magnetism of the 112 type iron pnictide compound [Formula: See text]. Sci. Rep. **11**(1), 12113 (2021)
39. Al-Sharif, A., AlAderah, B., Obeidat, A., Talla, J.: Influence of transition metal defects on electronic and magnetic properties of bulk silicon: ab-initio simulation. Mater. Today Commun. **34** (2023)
40. Karan, N.S., Sarma, D.D., Kadam, R.M., Pradhan, N.: Doping transition metal (Mn or Cu) ions in semiconductor nanocrystals. J. Phys. Chem. Lett. **1**(19), 2863–2866 (2010)
41. Liu, G., Tuttle, B.R., Dhar, S.: Silicon carbide: a unique platform for metal-oxide-semiconductor physics. Appl. Phys. Rev. **2**(2) (2015)
42. Talla, J.A., Alzrigat, M.S.: Effect of titanium impurity on electronic properties of double-walled nanotubes: theoretical approach. Russ. J. Inorg. Chem. **67**(11), 1888–1899 (2022)
43. Talla, J.A.: Stability and electronic properties of hybrid coaxial carbon nanotubes–boron nitride nanotubes under the influence of electric field, Appl. Phys. A **127**(8) (2021)
44. Shi, Z., Zhang, Z., Kutana, A., Yakobson, B.I.: Predicting two-dimensional silicon carbide monolayers. ACS Nano **9**(10), 9802–9809 (2015)
45. Zhou, B., Zhou, B., Liu, P., Zhou, G.: The giant Stark effect in armchair-edge phosphorene nanoribbons under a transverse electric field. Phys. Lett. A **382**(4), 193–198 (2018)
46. Brown, S.N.: Metrical oxidation states of 2-amidophenoxide and catecholate ligands: structural signatures of metal-ligand pi bonding in potentially noninnocent ligands. Inorg. Chem. **51**(3), 1251–1260 (2012)
47. Sarkar, T., Prakasha, K.R., Bharadwaj, M.D., Prakash, A.S.: Role of transition metals in a charge transfer mechanism and oxygen removal in Li(1.17)ni(0.17)mn(0.5)Co(0.17)O(2): experimental and first-principles analysis. Phys. Chem. Chem. Phys. **20**(29), 19606–19613 (2018)

48. Chhowalla, M., Shin, H.S., Eda, G., Li, L.J., Loh, K.P., Zhang, H.: The chemistry of two-dimensional layered transition metal dichalcogenide nanosheets. Nat. Chem. **5**(4), 263–275 (2013)
49. Mendez-Galvan, M., Celaya, C.A., Jaramillo-Quintero, O.A., Muniz, J., Diaz, G., Lara-Garcia, H.A.: Tuning the band gap of M-doped titanate nanotubes (M = fe, Co, Ni, and Cu): an experimental and theoretical study. Nanoscale Adv. **3**(5), 1382–1391 (2021)
50. Norton, D.P., Pearton, S.J., Hebard, A.F., Theodoropoulou, N., Boatner, L.A., Wilson, R.G.: Ferromagnetism in Mn-implanted ZnO:Sn single crystals. Appl. Phys. Lett. **82**(2), 239–241 (2003)